

1
2
3
4
5
6
7
8
9
10
11
12

Supplementary Information

Fabrication of Multi-functional Molecular Tunnelling Junctions by Click Chemistry

Ningyue Chen ^a, Zhenyu Yang ^a, Jin-Liang Lin ^a, Ziming Zhou ^a, Yu Xie ^a, Lejia

Wang^b and Yuan Li^{a*}

^a *Key Laboratory of Organic Optoelectronics and Molecular Engineering, Department
of Chemistry, Tsinghua University, Beijing 100084, China*

^b *School of Materials and Chemical Engineering, Ningbo University of Technology,
Ningbo 315211, China*

13

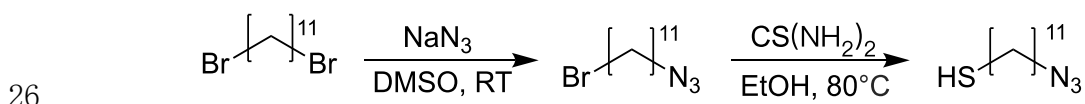
14 1 Materials and Synthesis

15 1.1 Materials and Characterizations

16 All commercial reagents and solvents were used as received without further
17 purification unless otherwise mentioned. Column chromatography was performed with
18 silica gel (pore size 60 Å, 230-400 mesh particle size) and thin layer chromatography
19 (TLC) was performed on silica gel with GF254 indicator. All yields given refer to
20 isolated yields unless otherwise noted. Nuclear magnetic resonance (NMR) spectra
21 were recorded on a 400 MHz Bruker spectrometer. Chemical shifts were reported in
22 ppm. Coupling constants (J values) were reported in Hertz. ¹H NMR chemical shifts
23 were referenced to CHCl₃ (7.26 ppm).

24

25 1.2 Synthesis and characterization of N₃(CH₂)₁₁SH

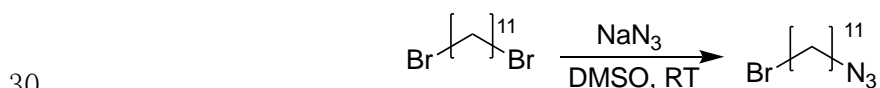


27

Figure S1. The synthetic route of target molecule N₃(CH₂)₁₁SH.

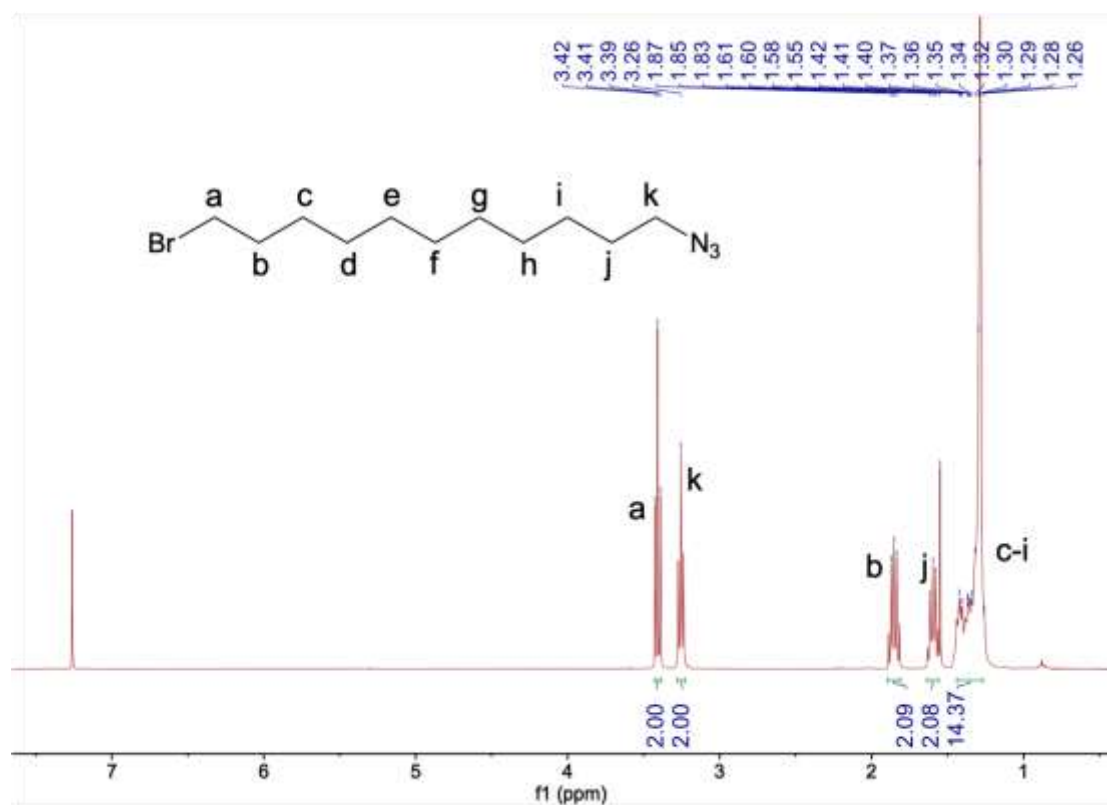
28 Synthesis

29 Compound N₃(CH₂)₁₁Br



31 We synthesized N₃(CH₂)₁₁Br according to a procedure reported in the literature¹. A
32 round-bottom flask was used to add with 1,11-dibromoundecane (2.0 g, 6.37 mmol)
33 and sodium azide (0.42 g, 6.37 mmol). To the solid mixture was added DMSO (35 mL).

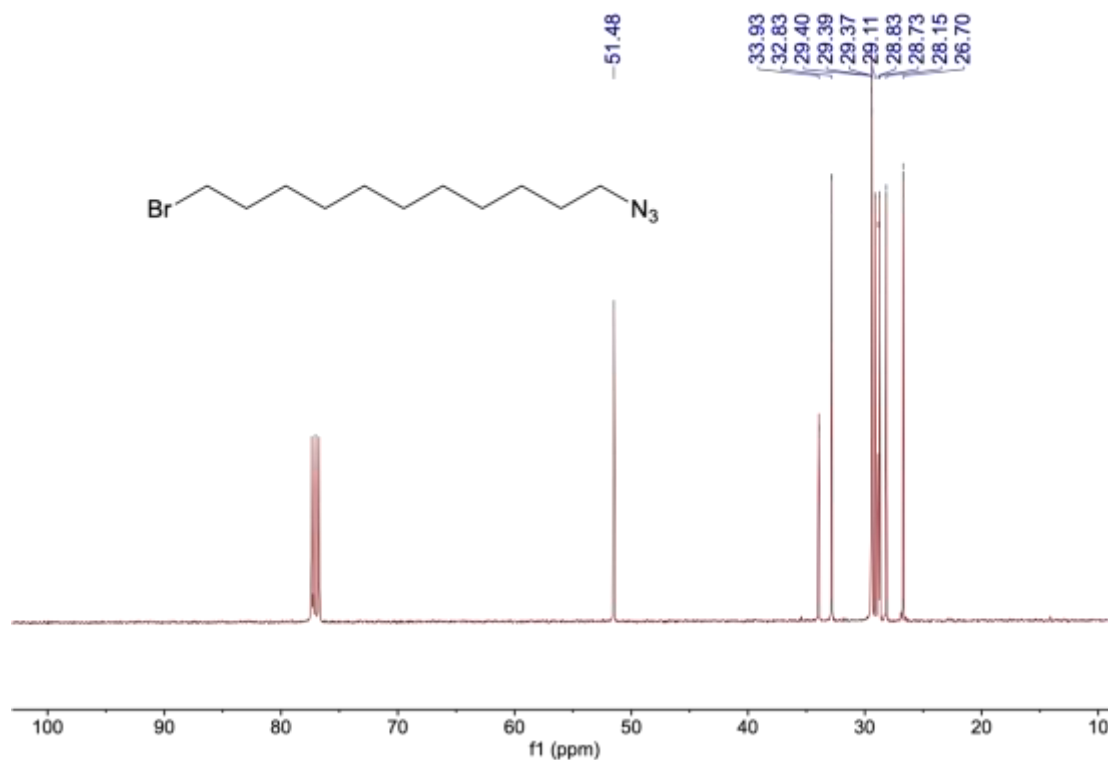
34 The solution was stirred vigorously at room temperature for 8 h. The solution was
35 diluted with water (30 mL). The aqueous phase was extracted with ether (3×30 mL)
36 and the combined organic phase was washed with water (2×20 mL), dried over MgSO_4 ,
37 filtered, and concentrated under reduced pressure. The reaction mixture was purified
38 by flash chromatography to afford the desired product as a colorless oil. ^1H NMR (400
39 MHz, CDCl_3) δ 3.41 (t, $J = 6.9$ Hz, 2H), 3.26 (s, 2H), 1.65 – 1.54 (m, 4H), 1.48 – 1.23
40 (m, 14H). ^{13}C NMR (101 MHz, CDCl_3) δ 51.48, 33.93, 32.83, 29.40, 29.39, 29.37,
41 29.11, 28.83, 28.73, 28.15, 26.70. TOF-MS m/z calc for $\text{C}_{11}\text{H}_{23}\text{N}_3\text{Br}$ $[\text{M}+\text{H}]^+$ 276.1075,
42 found 276.1061.



43

44

Figure S2 The ^1H -NMR spectrum of $\text{N}_3(\text{CH}_2)_{11}\text{Br}$.

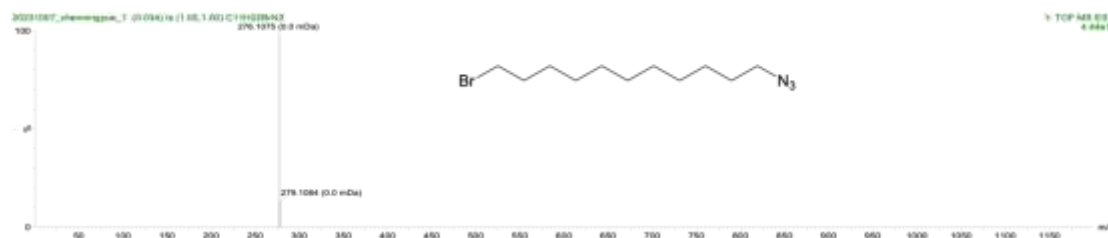


45

Figure S3 The ^{13}C -NMR spectrum of $\text{N}_3(\text{CH}_2)_{11}\text{Br}$.

46

47



48

Figure S4 The HRMS spectrum of $\text{N}_3(\text{CH}_2)_{11}\text{Br}$.

49

50

Compound $\text{N}_3(\text{CH}_2)_{11}\text{SH}$

51

We synthesized $\text{N}_3(\text{CH}_2)_{11}\text{SH}$ according to a procedure reported in the literature².

52

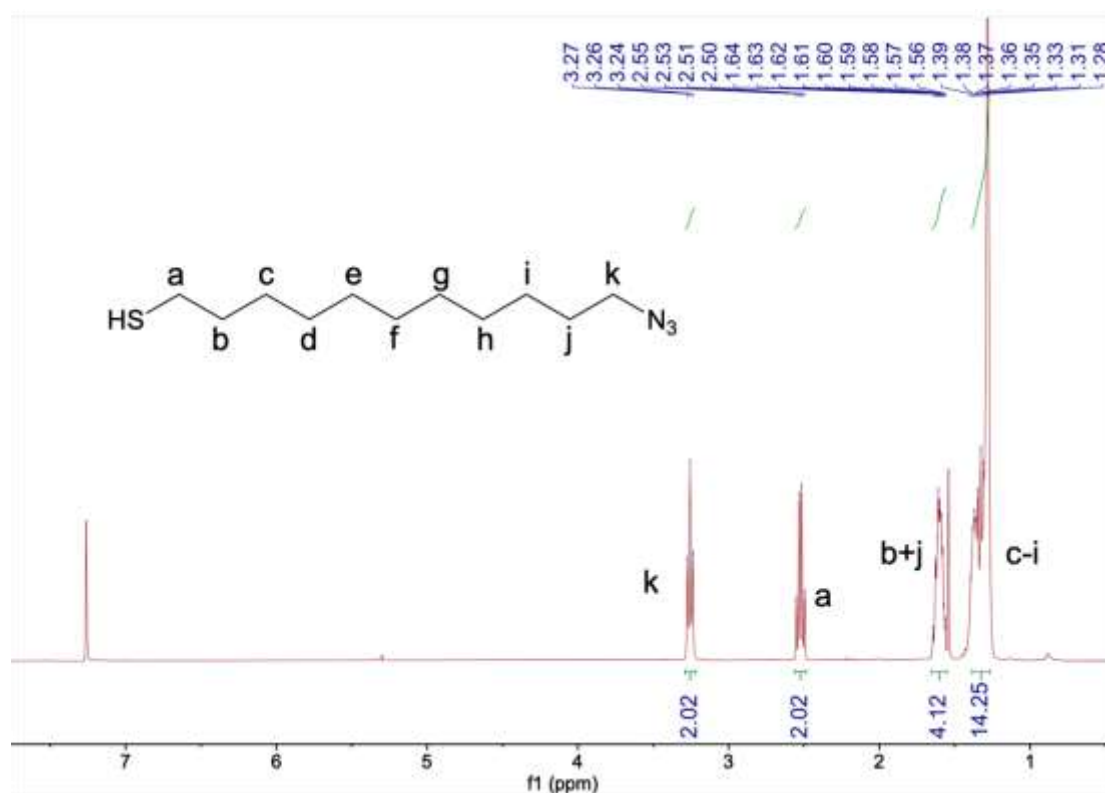
The compound $\text{Br}(\text{CH}_2)_{11}\text{N}_3$ (6.5 g, 23 mmol) was added to a solution of $\text{CS}(\text{NH}_2)_2$

53

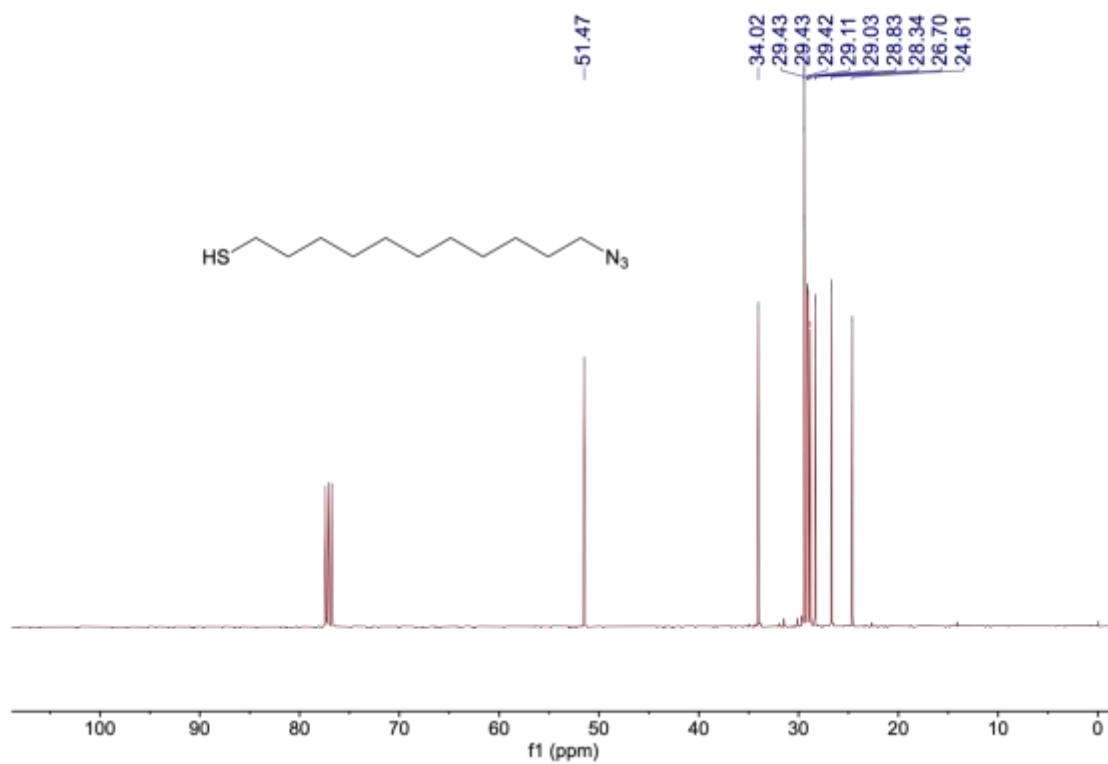
(1.75 g, 24 mmol) in ethanol (50 mL). The mixture was stirred for 16 h at 80 °C. To

54

55 this mixture was then added a NaOH solution (10 mL, 3 M). After stirring for 5 min at
56 ambient temperature, the final mixture was neutralized with H₂SO₄ solution (20 mL,
57 3M), and was stirred for 20 min at ambient temperature. All volatiles were removed.
58 The crude was extracted with CH₂Cl₂ (4×50 mL), and the extract was dried to give
59 N₃(CH₂)₁₁SH as a transparent liquid. ¹H NMR (400 MHz, CDCl₃) δ 3.26 (t, *J* = 7.0 Hz,
60 2H), 2.52 (q, *J* = 7.4 Hz, 2H), 1.66 – 1.55 (m, 4H), 1.41 – 1.26 (m, 14H). ¹³C NMR
61 (101 MHz, CDCl₃) δ 51.47, 34.02, 29.43, 29.43, 29.42, 29.11, 29.03, 28.83, 28.34,
62 26.70, 24.61. TOF-MS *m/z* calc for C₁₁H₂₂N₃S [M-H]⁺ 228.1534, found 228.1528.



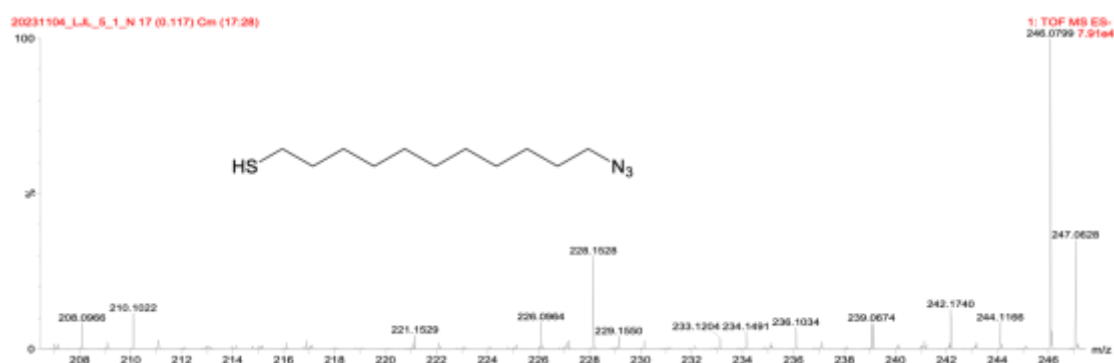
64 **Figure S5** The ¹H-NMR spectrum of N₃(CH₂)₁₁SH.



65

66

Figure S6 The ^{13}C -NMR spectrum of $\text{N}_3(\text{CH}_2)_{11}\text{SH}$.



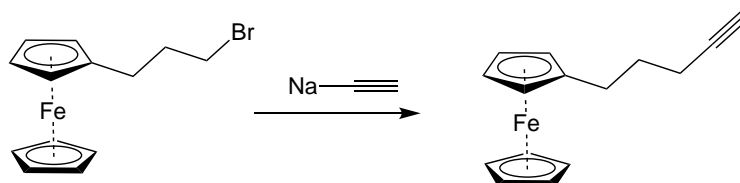
67

68

Figure S7 The HRMS spectrum of $\text{N}_3(\text{CH}_2)_{11}\text{SH}$.

69

70 1.3 Synthesis and characterization of $\text{FcC}_3\text{-CC}$



71

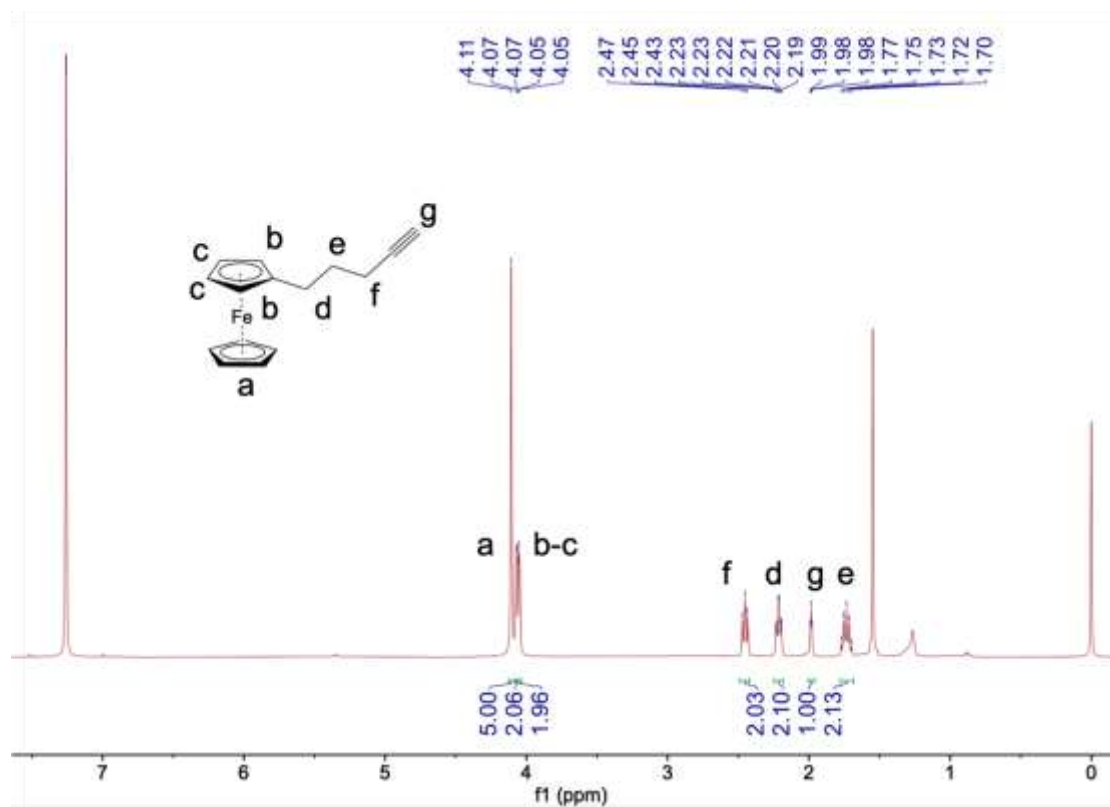
72 **Figure S8.** The synthetic route of target molecule FcC₃-CC.

73 **Synthesis**

74 FcC₃Br (307 mg, 1 mmol) was dissolved in 10 mL dimethylformamide. At 0°C
75 sodium acetylide (410ml (18 weight-% slurry in xylene), 1.3 mmol, 1.3 eq.) was slowly
76 added, and the mixture was stirred for 1h. After complete conversion, monitored by TLC,
77 2 mL water was added. The solvent was removed in vacuo, and the residue was
78 dissolved in water (100 mL) and hexane (30 mL). Layers were separated, and the
79 aqueous layer was extracted three times with hexane (20 mL). After drying the solution
80 over Na₂SO₄, filtration through silica gel (pentane/toluene, 9/1) and evaporation of the
81 solvent, the product was obtained as an orange oil. ¹H NMR (400 MHz, CDCl₃) δ 4.11
82 (s, 5H), 4.09 – 4.06 (m, 2H), 4.06 – 4.04 (m, 2H), 2.45 (t, J = 7.7 Hz, 2H), 2.21 (td, J =
83 7.1, 2.6 Hz, 2H), 1.98 (d, J = 2.7 Hz, 1H), 1.73 (p, J = 7.3 Hz, 2H). ¹³C NMR (101 MHz,
84 CDCl₃) δ 88.18, 84.43, 68.56, 68.14, 67.24, 29.71, 28.51, 18.21. TOF-MS m/z calc for
85 C₁₅H₁₆Fe [M]⁺ 252.0601, found 252.062.

86

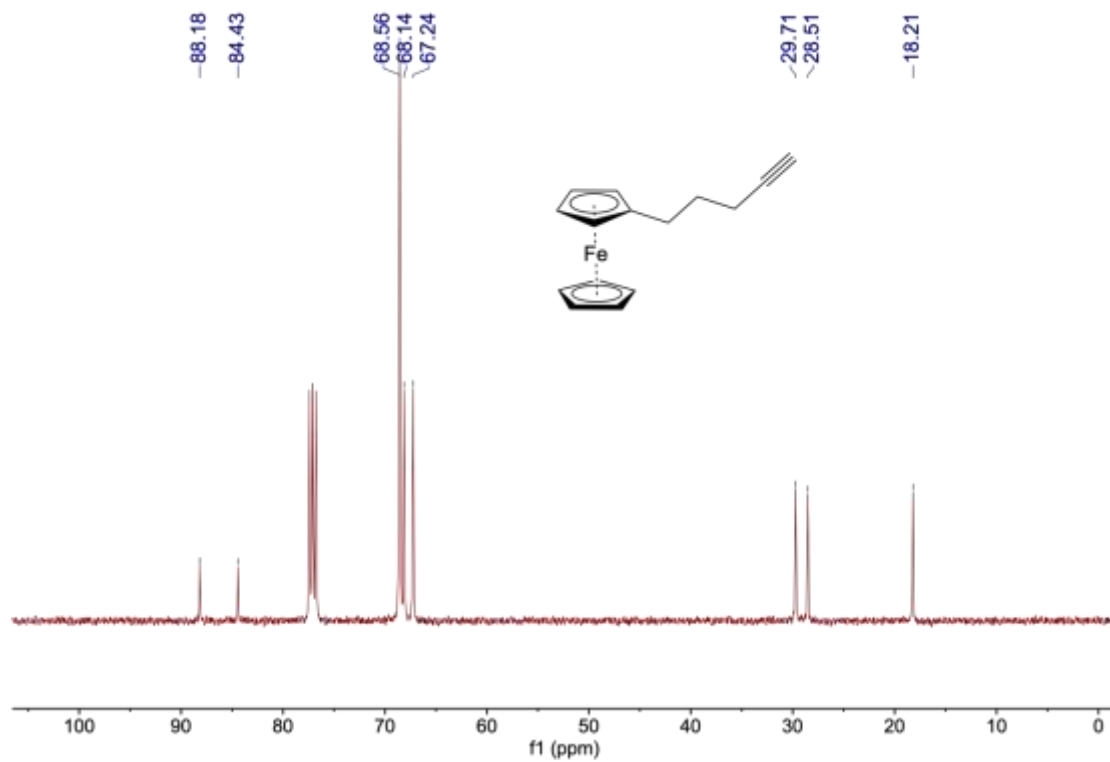
87



88

89

Figure S9. The ¹H-NMR spectrum of FcC₃-CC.

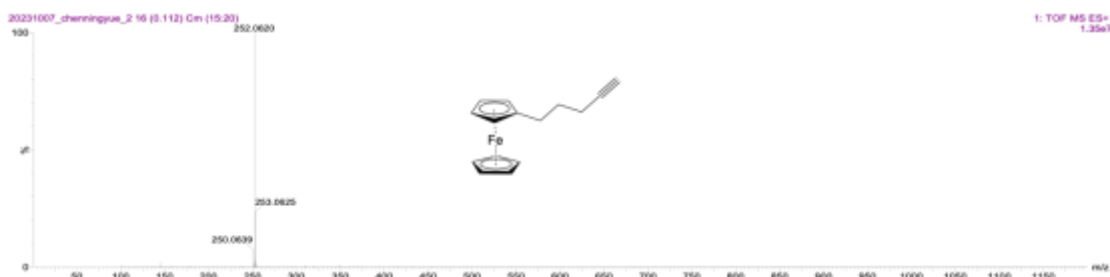


90

91

Figure S10. The ¹³C-NMR spectrum of FcC₃-CC.

92

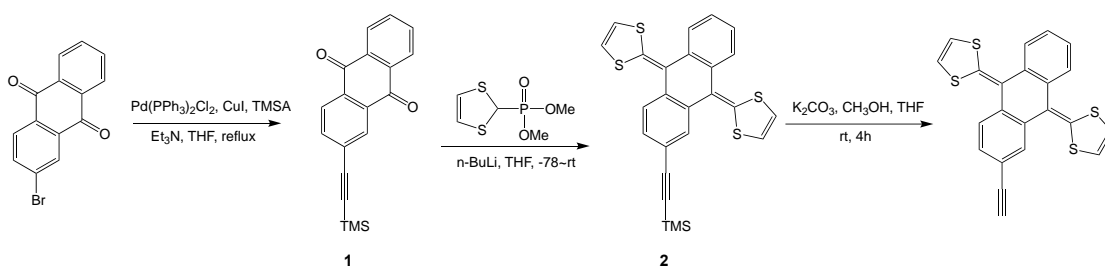


93

94

Figure S11 The HRMS spectrum of FcC₃-CC.

95 1.4 Synthesis and characterization of exTTF-CC³



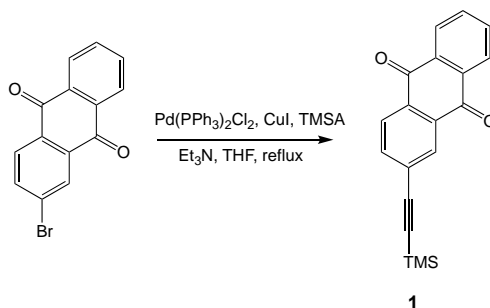
96

97

Figure S12. The synthetic route of target molecule exTTF-CC.

98 **Synthesis**

99 **Compound 1**

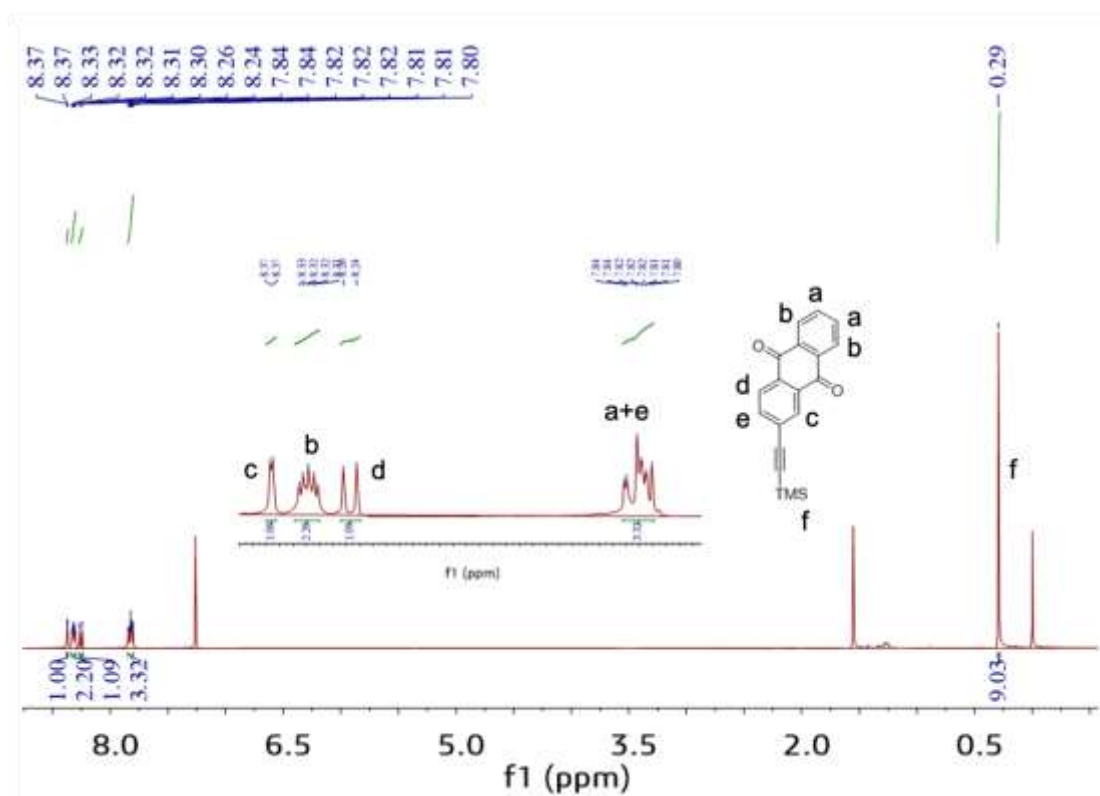


100

101 2-bro-moanthraquinone (0.29 g, 1.0 mmol), trimethylsilylacetylene (0.22 mL, 1.5
 102 mmol), Pd(PPh₃)₂Cl₂ (55 mg, 0.05 mmol), and CuI (30 mg, 0.05 mmol), anhydrous
 103 triethylamine (15 mL), anhydrous THF (15 mL) were added into a 100 mL Schlenk
 104 tube. After degassing by bubbling with N₂ for 15 min, the mixture was then heated at
 105 85 °C for 12 h under N₂ atmosphere. After the mixture was cooled down to room
 106 temperature, the solvents were removed in vacuo. The crude product was then purified
 107 by column chromatography (silica gel, CH₂Cl₂/petroleum ether = 1/4 v/v) and
 108 recrystallized from CHCl₃/CH₃OH to obtain pure product as light-yellow solids. Yield:

109 274 mg, 90%. ^1H NMR (400 MHz, CDCl_3) δ 8.37 (d, $J = 1.6$ Hz, 1H), 8.34 – 8.30 (m,
110 2H), 8.25 (d, $J = 8.0$ Hz, 1H), 7.85 – 7.79 (m, 3H), 0.29 (s, 9H). ^{13}C NMR (101 MHz,
111 CDCl_3) δ 182.54, 182.50, 136.92, 134.37, 134.28, 133.58, 133.46, 133.40, 132.57,
112 130.74, 129.44, 127.41, 127.37, 127.33, 103.31, 100.24, 0.11. TOF-MS m/z calc for
113 $\text{C}_{19}\text{H}_{16}\text{O}_2\text{Si}$ $[\text{M}+\text{H}]^+$ 305.0998, found 305.1017.

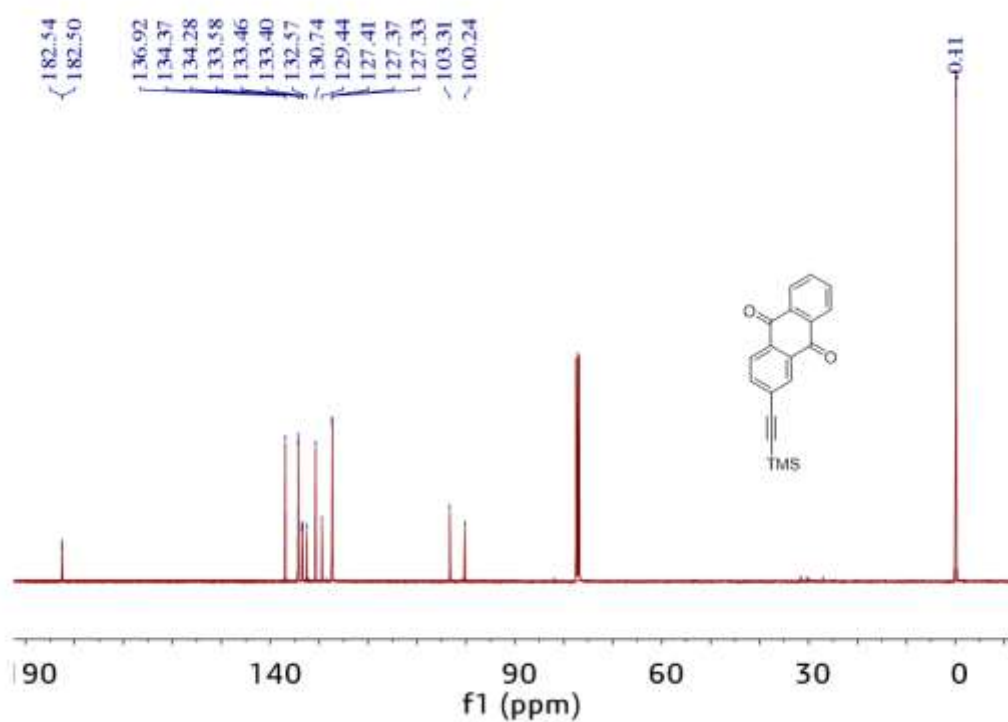
114



115

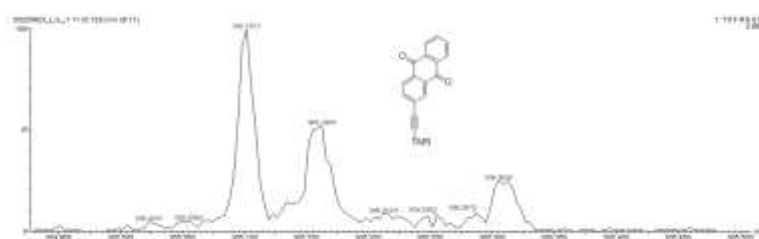
116

Figure S13 The ^1H -NMR spectrum of compound **1**.



117
118

Figure S14. The ^{13}C -NMR spectrum of compound **1**.



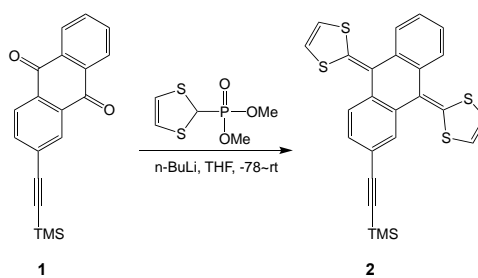
119

120

Figure S15. The HRMS spectrum of compound **1**.

121

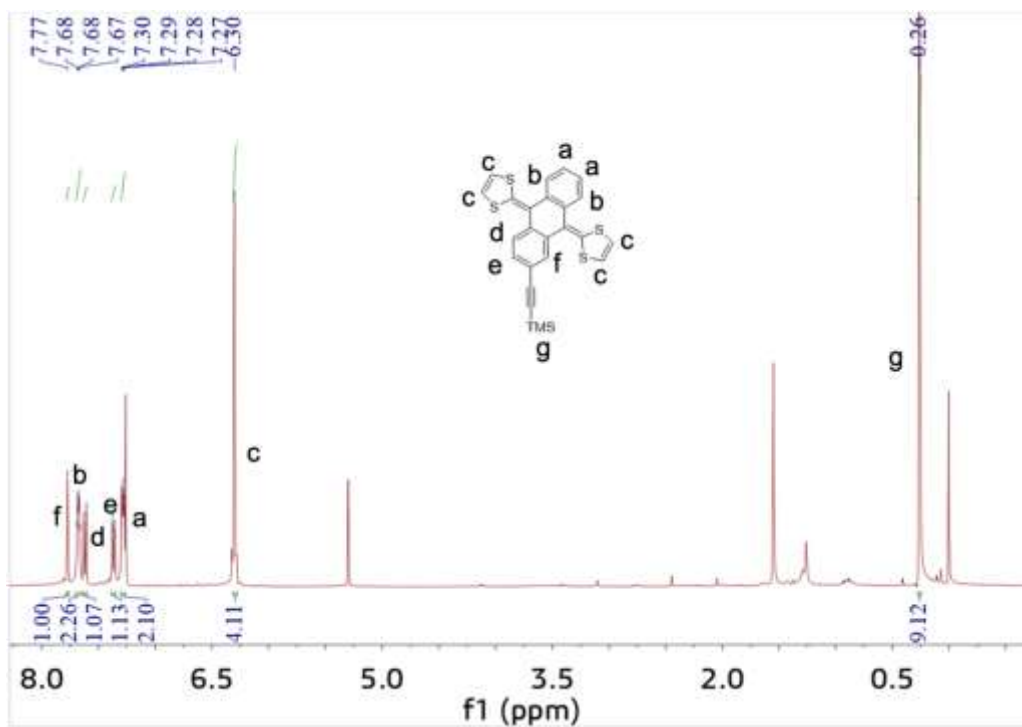
122 **Compound 2**



123

124 To a solution of dimethyl 1,3-dithiol-2-yl-2-phosphonate (1.00 g, 4.72 mmol) in
125 dry THF (50 mL) at -78°C under N₂ atmosphere, n-BuLi (1.6 M, 1.90 ml, 4.72 mmol)
126 was added over a period of 10 min. After 0.5h at -78°C, the compound **1** (0.57 g, 1.89
127 mmol), suspended in dry THF (50 mL), was added dropwise into the solution of the
128 phosphonate. The mixture was stirred for an additional hour at -78°C, then allowed to
129 warm to room temperature, and then left to stand overnight at room temperature. The
130 THF was evaporated under reduced pressure and water (100 mL) was added. The
131 residue was extracted with CH₂Cl₂, (3×100 ml) and the combined organic layers were
132 dried over Na₂SO₄, filtered and the solvent was removed under reduced pressure. The
133 crude product was then purified by column chromatography (silica gel, CH₂Cl₂/
134 hexanes = 1/4 v/v) and obtained a pure product as yellow solids (586 mg, 65%). ¹H
135 NMR (400 MHz, CDCl₃) δ 7.77 (s, 1H), 7.71 – 7.65 (m, 2H), 7.62 (d, J = 8.0 Hz, 1H),
136 7.37 (dd, J = 8.0, 1.4 Hz, 1H), 7.28 (dd, J = 5.6, 3.3 Hz, 2H), 6.30 (s, 4H), 0.26 (s, 9H).
137 ¹³C NMR (101 MHz, CDCl₃) δ 136.81, 136.68, 135.66, 135.50, 135.33, 129.66, 128.31,
138 126.20, 126.18, 125.11, 125.02, 124.97, 121.83, 121.37, 120.64, 117.43, 117.40,
139 117.30, 105.46, 94.47, 0.19. TOF-MS m/z calc for C₂₅H₂₀S₄Si [M]⁺ 476.0217, found
140 476.0194.

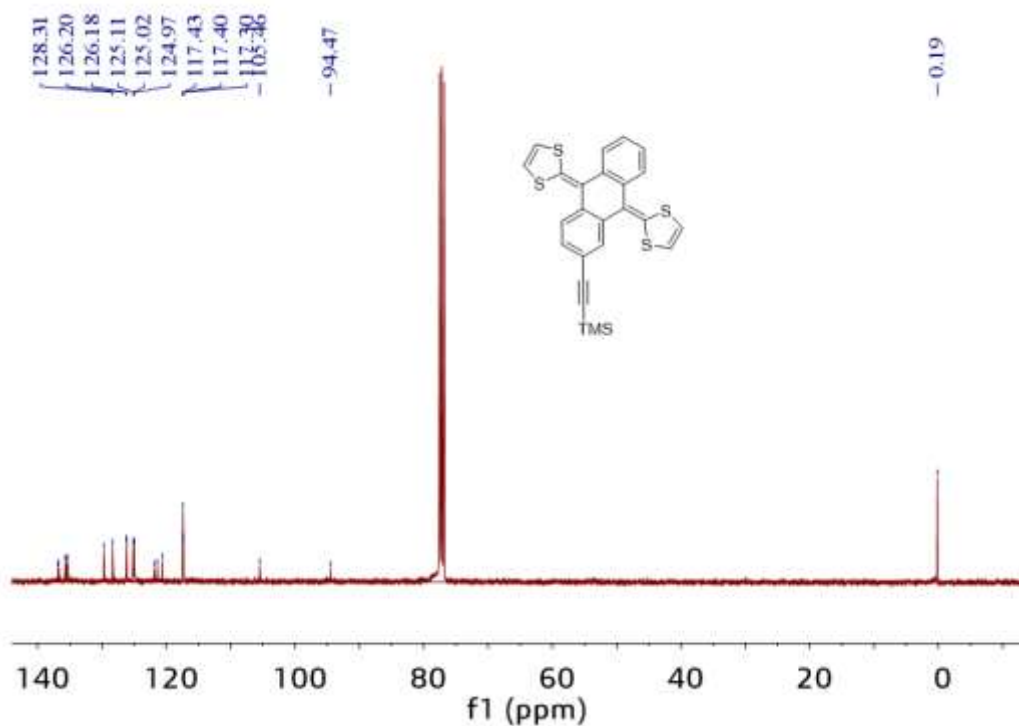
141



142

143

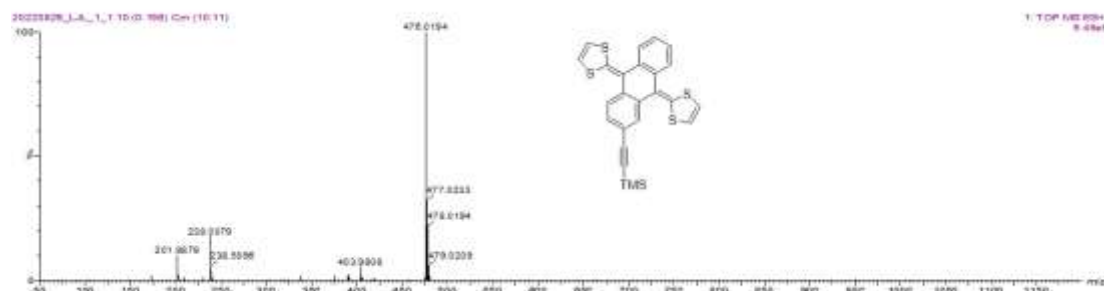
Figure S16. The ^1H -NMR spectrum of compound **2**.



144

145

Figure S17. The ^{13}C -NMR spectrum of compound **2**.



146

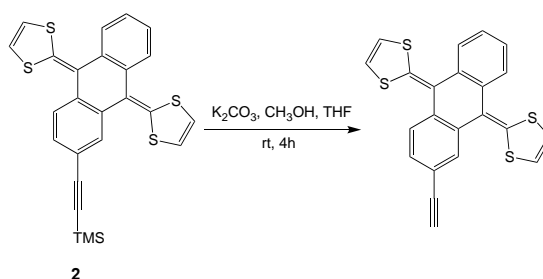
147

Figure S18. The HRMS spectrum of compound **2**.

148

149

exTTF-CC



150

151

A solution of compound **2** (143 mg, 0.3 mmol) in THF/CH₃OH (1:1, 20 mL) and

152

K₂CO₃ (40 mg, 0.3 mmol) was stirred at room temperature for 4 h. The mixture was

153

then extracted with CH₂Cl₂ (3×25 mL), and the combined organic layers were washed

154

with water (2×50 mL) and dried with Na₂SO₄. The residue was purified by flash

155

chromatography on silica gel using PE/CH₂Cl₂ (3:1) as the eluent to give compound

156

exTTF-CC (122 mg, 100%) as a yellow solid. ¹H NMR (400 MHz, CDCl₃) δ 7.81 (brs,

157

1H), 7.73 – 7.68 (m, 2H), 7.65 (d, J = 8.0 Hz, 1H), 7.40 (d, J = 8.0 Hz, 1H), 7.33 – 7.28

158

(m, 2H), 6.31 (s, 4H), 3.10 (s, 1H). ¹³C NMR (101 MHz, CDCl₃) δ 137.08, 136.91,

159

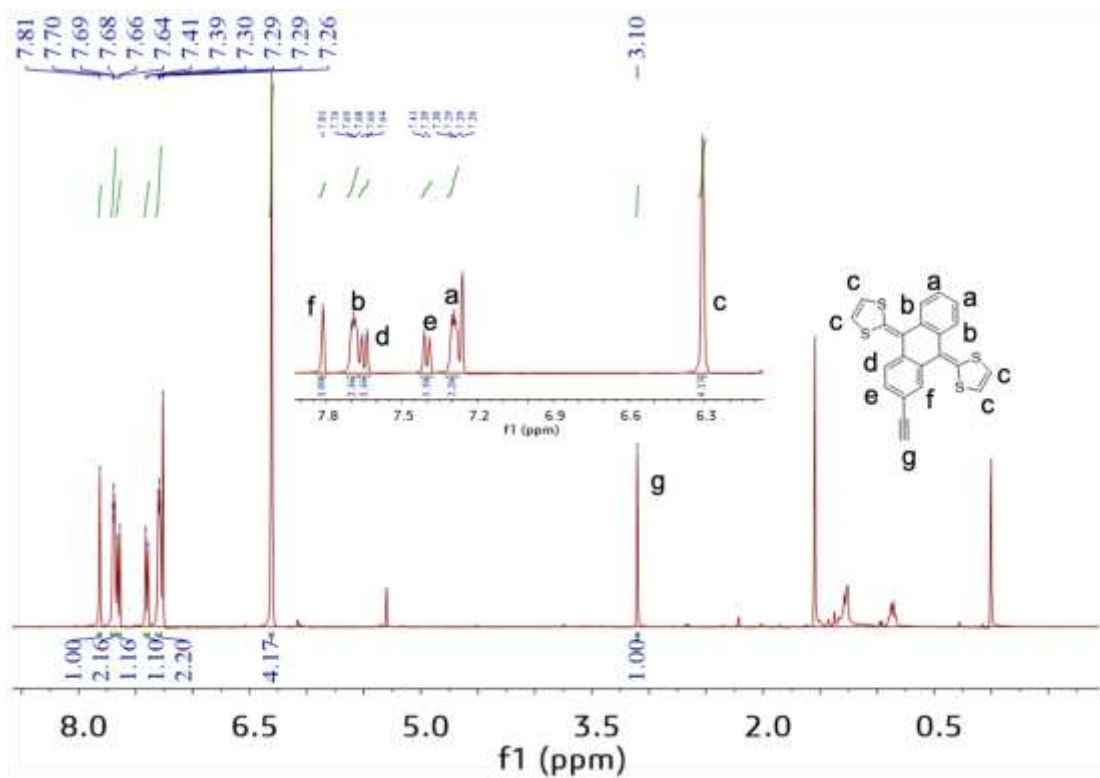
135.98, 135.60, 135.30, 129.73, 128.57, 126.25, 126.23, 125.11, 125.06, 125.04,

160

121.68, 121.20, 119.49, 117.45, 117.38, 117.31, 84.02, 77.38. TOF-MS m/z calc for

161

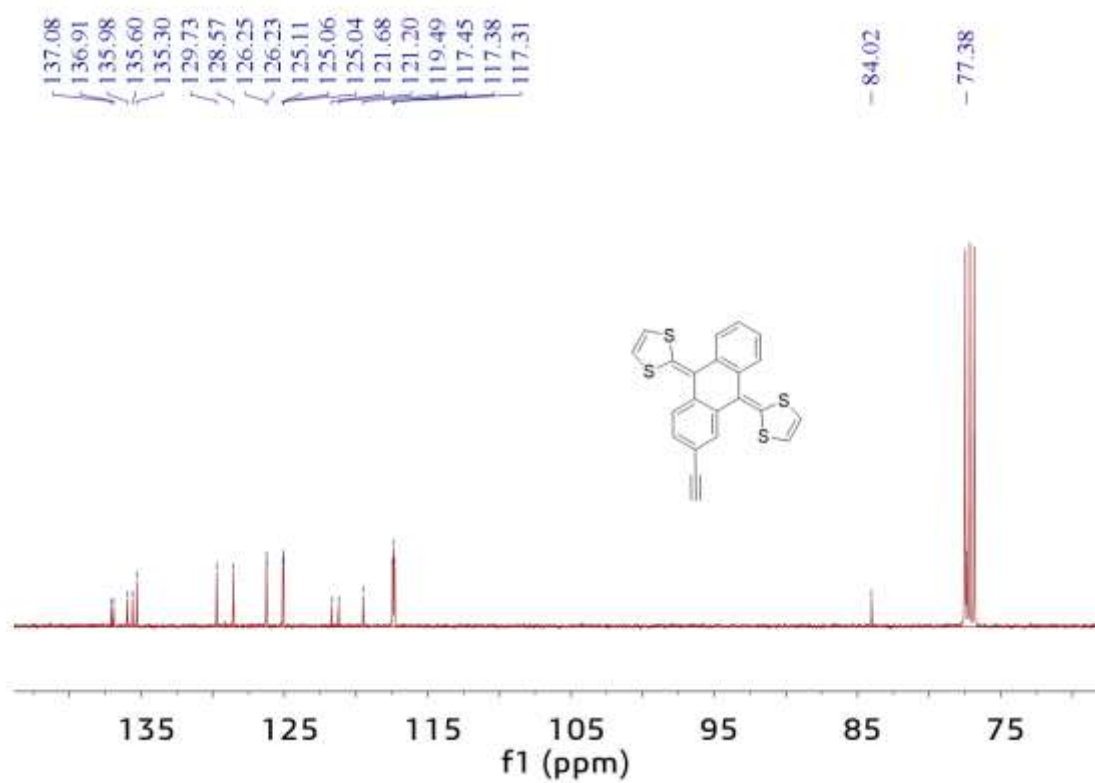
C₂₂H₁₂S₄ [M]⁺ 403.9822, found 403.9808.



162

163

Figure S19. The ^1H -NMR spectrum of exTTF-CC.



164

165

Figure S20. The ^{13}C -NMR spectrum of exTTF-CC.



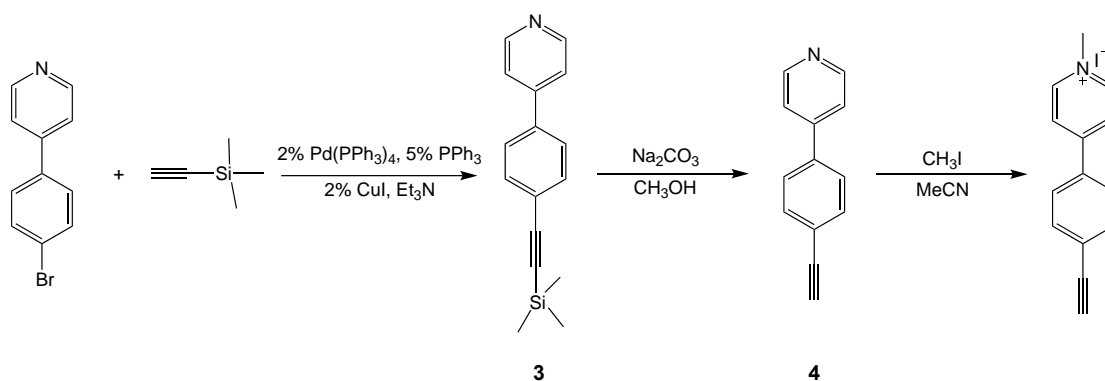
166

167

Figure S21. The HRMS spectrum of exTTF-CC.

168

169 1.5 Synthesis and characterization of I+MPP-CC

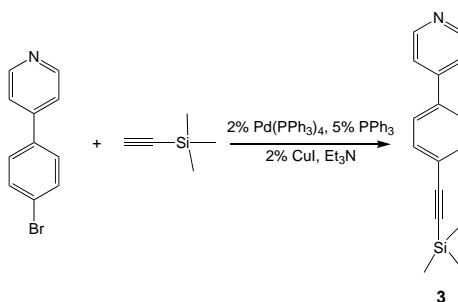


170

171

Figure S22. The synthetic route of target molecule I+MPP-CC

172 **Compound 3**



173

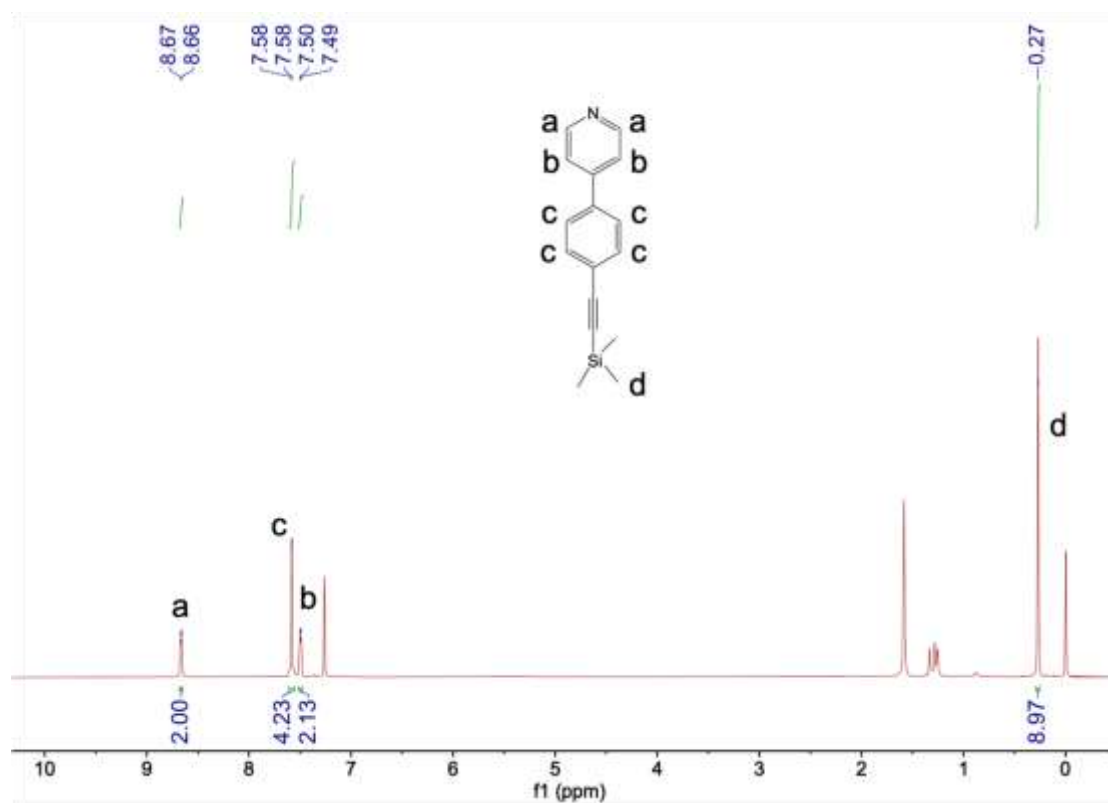
174 Ethynyltrimethylsilane (0.66 g, 6.7 mmol) in dry Et₃N was added dropwise to a
 175 suspension of 4-(4-bromophenyl) pyridine (1.31 g, 5.6 mmol), Pd(PPh₃)₄ (0.13 g, 0.11
 176 mmol), CuI (0.02 g, 0.11 mmol) and PPh₃ (0.07 g, 0.28 mmol) in dry Et₃N (50 mL) at
 177 room temperature. The solution was heated at 60 °C and stirred for 8 h. The mixture
 178 was then cooled and filtered, and DCM was added and the organic layer was washed

179 with saturated ammonium chloride solution, dried over anhydrous MgSO_4 and the
180 solvents were evaporated. The crude product was purified by column chromatography
181 using PE as eluent, to give a pale-yellow solid, yield 85%. ^1H NMR (400 MHz, CDCl_3)
182 δ 8.66 (d, $J = 4.2$ Hz, 2H), 7.58 (d, $J = 1.8$ Hz, 4H), 7.50 (d, $J = 4.3$ Hz, 2H), 0.27 (s,
183 9H). ^{13}C NMR (101 MHz, CDCl_3) δ 150.32, 147.46, 137.94, 132.67, 126.77, 124.06,
184 121.42, 104.36, 96.14, -0.08. TOF-MS m/z calc for $\text{C}_{16}\text{H}_{18}\text{NSi}$ $[\text{M}+\text{H}]^+$ 252.1209,
185 found 252.1205.

186

187

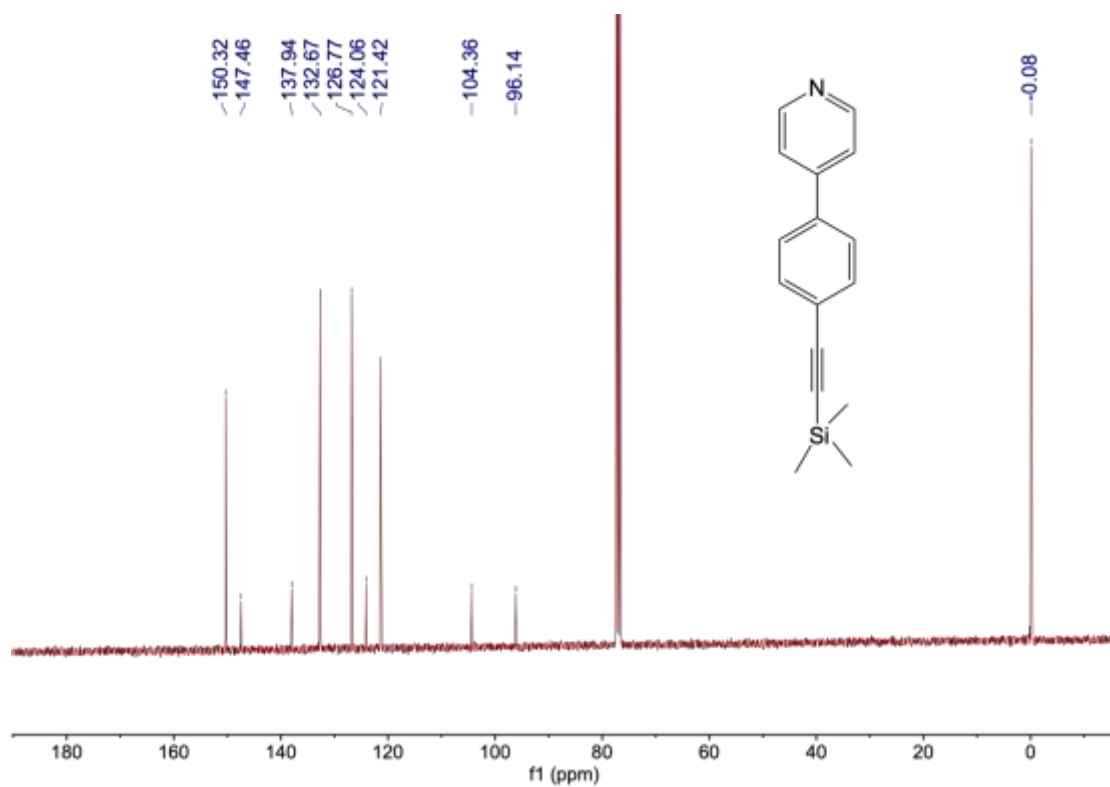
188



189

190

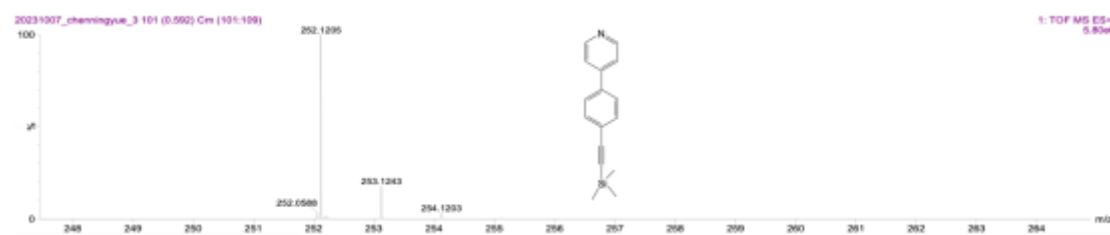
Figure S23. The ^1H -NMR spectrum of compound 3.



191

Figure S24. The ^{13}C -NMR spectrum of compound **3**.

192



193

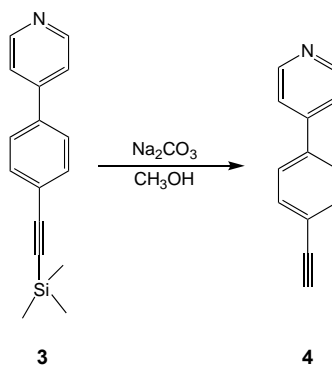
Figure S25. The HRMS spectrum of compound **3**.

194

195

196

Compound **4**



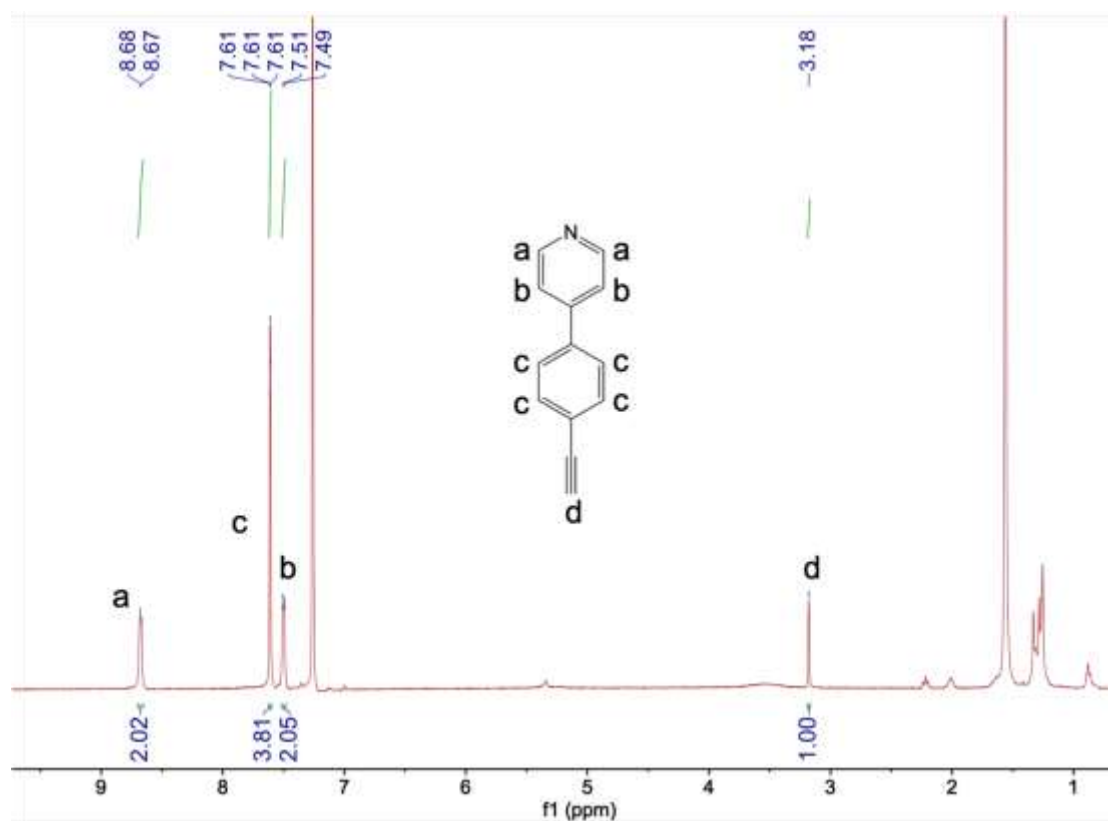
197

198 We synthesized compound **4** according to a procedure reported in the literature⁴.
199 A mixture of **3** (1.15 g, 4.6 mmol), potassium carbonate (1.9 g, 13.8 mmol), CH₃OH
200 (30 mL) was stirred for 4 h, and the reaction mixture was extracted with DCM, washed
201 with water and brine, and the combined organic layers were dried with MgSO₄. After
202 removing the solvent under reduced pressure, compound **4** was obtained as pale-yellow
203 solid without further purification. Yield: 99%. ¹H NMR (400 MHz, CDCl₃) δ 8.67 (d,
204 *J* = 4.3 Hz, 2H), 7.64 – 7.58 (m, 4H), 7.50 (d, *J* = 5.0 Hz, 2H), 3.18 (s, 1H). ¹³C NMR
205 (101 MHz, CDCl₃) δ 150.26, 147.50, 138.37, 132.86, 126.92, 123.04, 121.50, 83.01,
206 78.76. TOF-MS *m/z* calc for C₁₃H₁₀N [M+H]⁺ 180.0813, found 180.0814.

207

208

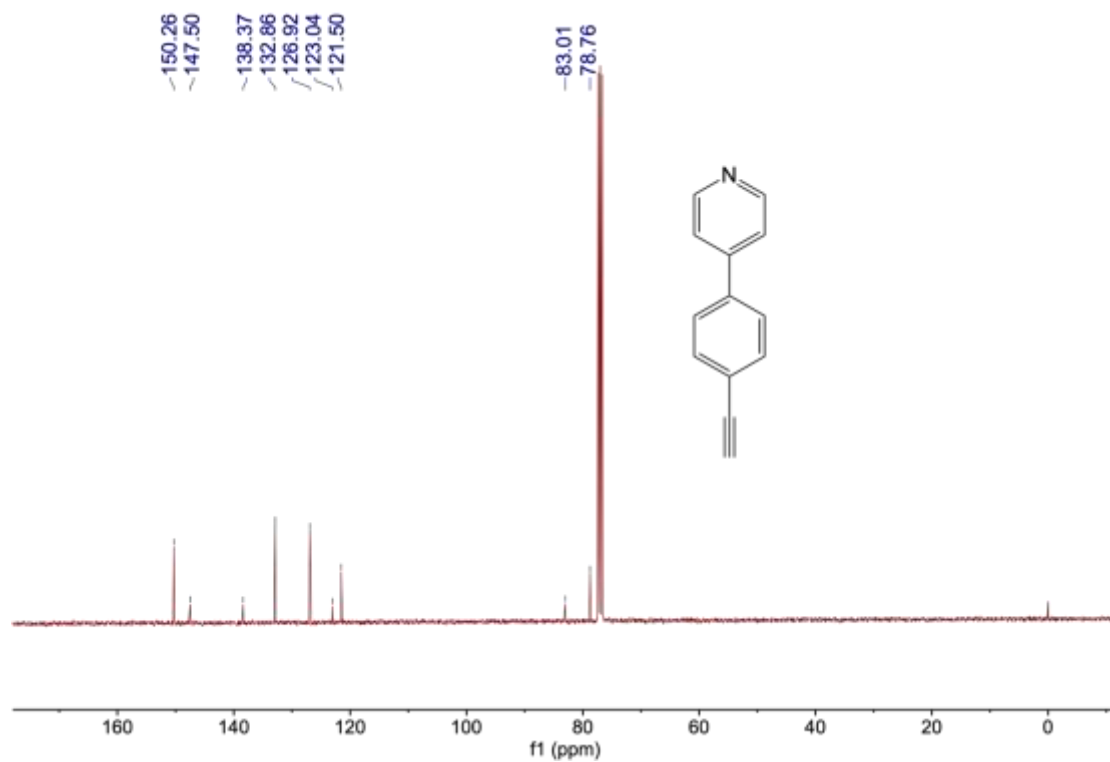
209



210

211

Figure S26. The ¹H-NMR spectrum of compound **4**.

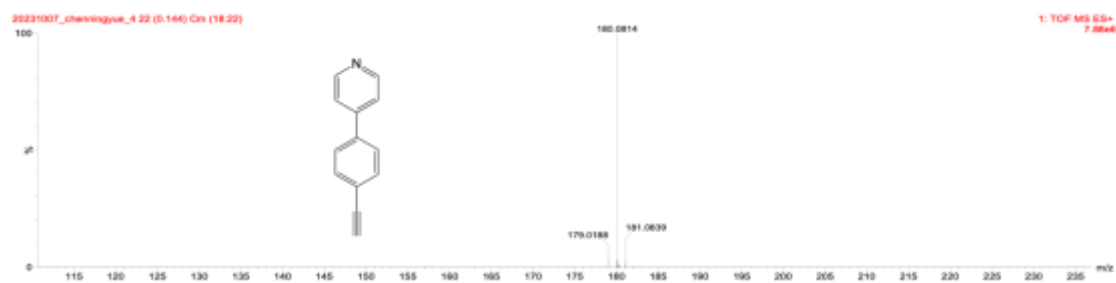


212

213

Figure S27. The ¹³C-NMR spectrum of compound **4**.

214



215

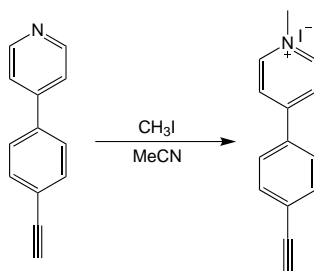
216

Figure S28. The HRMS spectrum of compound **4**.

217

218

I+MPP-CC

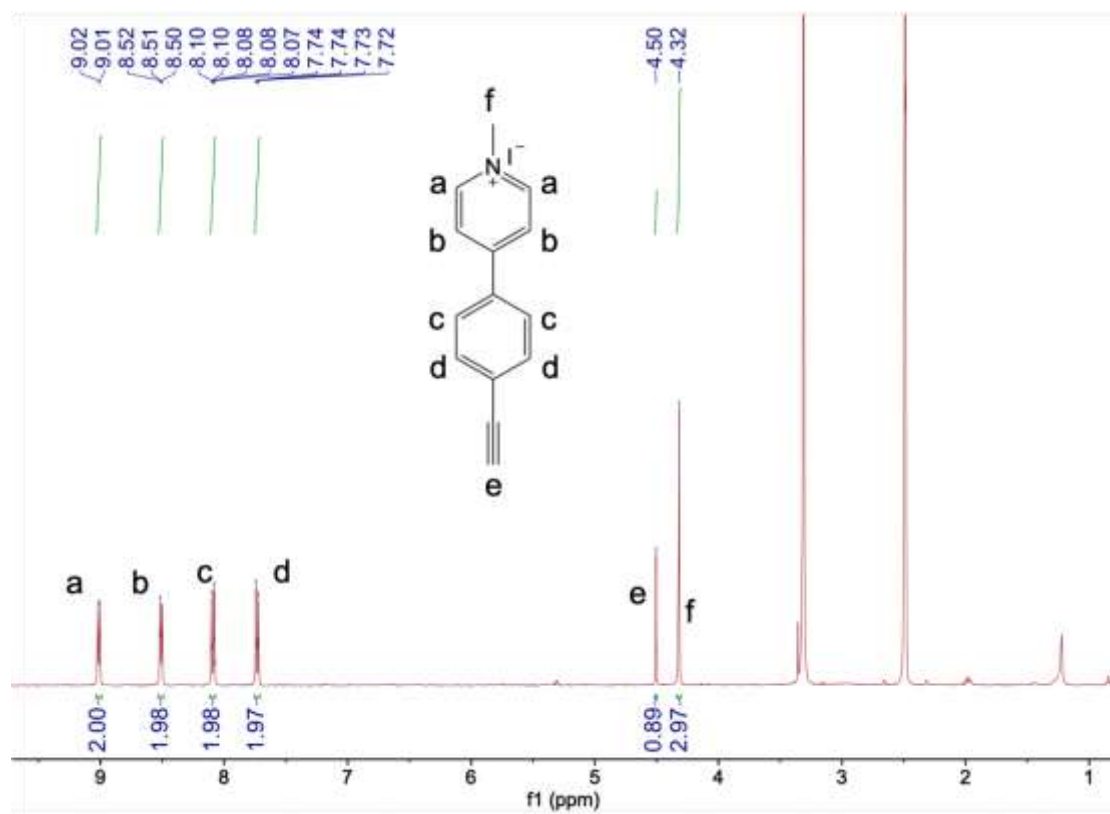


219

4

220 We synthesized I+MPP-CC according to a procedure reported in the literature⁵.
221 To the corresponding solution of **4** (5.0 mmol, 1.0 equiv.) in acetonitrile (5 mL) was
222 added iodoalkane (10 mmol, 2.0 equiv.) in a two-necked flask under nitrogen. The
223 reaction mixture was refluxed overnight. Then it was cooled to room temperature, and
224 the solvent was removed under reduced pressure to obtain the crude product, which was
225 recrystallized in MeCN/EtOAc co-solvent to afford a pure product. ¹H NMR (400 MHz,
226 DMSO) δ 9.01 (d, *J* = 6.6 Hz, 2H), 8.51 (d, *J* = 6.8 Hz, 2H), 8.12 – 8.05 (m, 2H), 7.76
227 – 7.70 (m, 2H), 4.50 (s, 1H), 4.32 (s, 3H). ¹³C NMR (101 MHz, DMSO) δ 153.68,
228 146.18, 134.21, 133.27, 128.82, 125.75, 124.70, 84.54, 83.09, 47.65. TOF-MS *m/z* calc
229 for C₁₄H₁₃NI [M+H]⁺ 322.0093, found 322.0101.

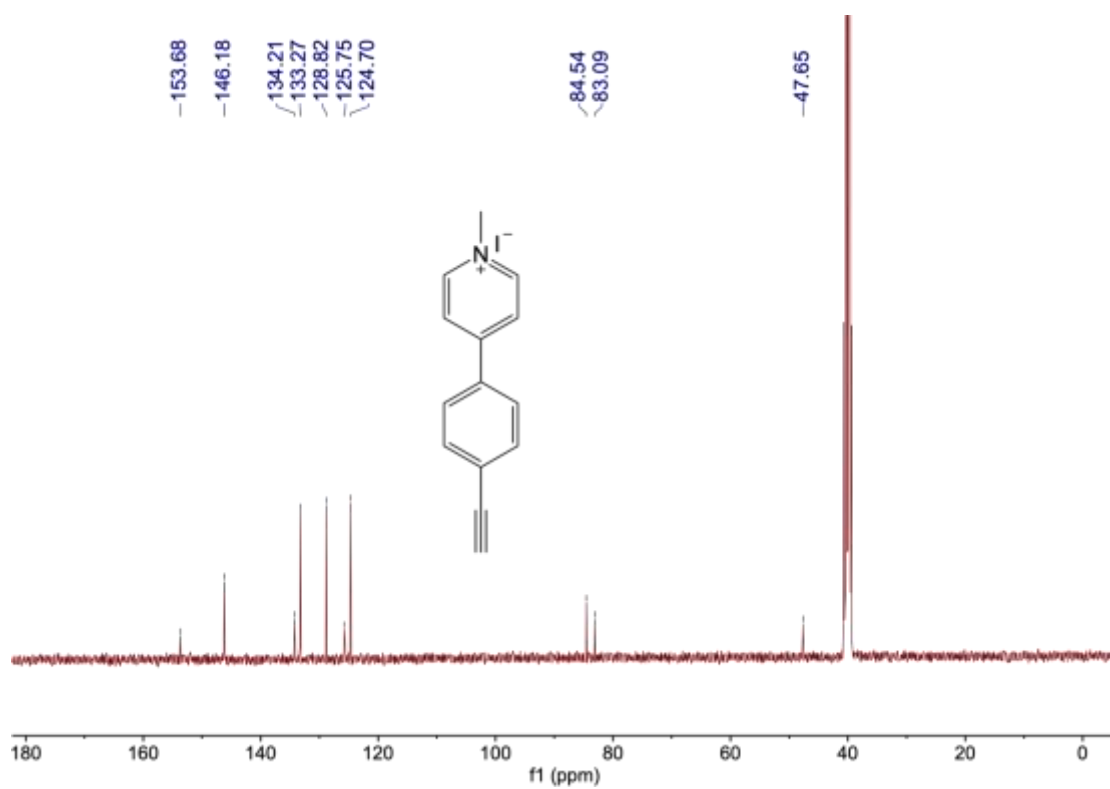
230



231

232

Figure S29. The ^1H -NMR spectrum of I+MPP-CC.

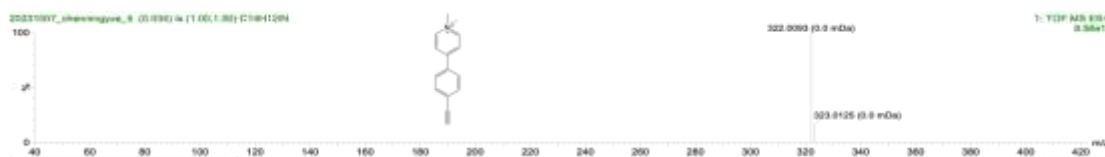


233

234

Figure S30. The ^{13}C -NMR spectrum of I+MPP-CC.

235



236

237

Figure S31. The HRMS spectrum of I+MPP-CC.

238

239 **2 SAMs preparation**

240 **2.1 Fabrication and characterization of template-stripped bottom electrodes.**

241 We fabricated the template-stripped bottom electrodes following the previous
242 reports³. We used gold pellets (0.125" (diameter) × 0.125" (length)) with the purity of
243 99.999% obtained from Dimu Materials, Inc (China). Silicon (100, p-type) wafers are
244 from KST (Japan), with a thickness of $525 \pm 25 \mu\text{m}$ with one side polished. We used a
245 thermal evaporator (Shen Yang Ke Yi, China) to deposit Au vapour on top of polished
246 surfaces of Si/SiO₂ wafers. The vacuum of deposition was about 8×10^{-5} Pa, and the
247 evaporation rate was about 0.2 Å/s at the first 50 nm and then increased to ~1.0 Å/s for
248 the rest 150 nm. The glass slides ($1.5 \times 1.5 \text{ cm}^2$) were ultrasonically cleaned with
249 acetone and then ethanol for 20 minutes, and the slides were blown to dryness in a
250 stream of N₂ gas. After we cleaned the glass slides with a plasma of air for 5 mins at a
251 pressure of 100 Pa, the glass slides were glued on the Au surfaces by photo-curable
252 optical adhesive (Norland, No. 61). A 100-Watt UV lamp was used to cure the optical
253 adhesive for 1 hour at a distance of 60 cm from the light source. The Au surface that
254 had been in contact with the Si/SiO₂ wafer was lifted off by a razor blade.

255

256 **2.2 Fabrication of N₃-SAMs**

257 To prepare the basic SAMs for click reaction, we formed the N₃-terminated SAMs
258 (N₃-SAMs) by immersing freshly prepared template-stripped Au (Au^{TS}) substrates⁶ into
259 a solution of 1.0 mM N₃(CH₂)₁₁SH in absolute ethanol. Following a 3-hour immersion

260 period, the N₃-SAMs samples were meticulously rinsed with pure ethanol and
261 subsequently dried with nitrogen gas. After these steps, the N₃(CH₂)₁₁SH molecules
262 were primed for assembly onto the gold substrates through a thiol-Au reaction, forming
263 N₃-SAMs.

264

265 **2.3 Fabrication of clicked-SAMs**

266 To immobilize organic functional groups including Fc, C₃-Fc and exTTF, we
267 immersed N₃-SAMs in a DMF solution containing 1.0 mM CuSO₄·5H₂O, 100.0 mM
268 ascorbic acid (AA), and 10.0 mM functional group molecules, with a ratio of
269 CuSO₄·5H₂O/AA/functional groups 1:1:4 in volume ratio for 24h⁷. To prevent
270 potential photooxidation of the SAMs, we stored the samples in a dark, room-
271 temperature environment under a nitrogen atmosphere. After the reaction was
272 completed, we sequentially rinsed the samples with ethanol and dichloromethane to
273 remove the physisorbed functional groups yielding Fc-SAMs, Fc-C₃-SAMs and
274 exTTF-SAMs respectively.

275 Meanwhile, for ion-type functional groups MPP+I, the click reaction was
276 performed in EtOH/H₂O (3:1 in volume ratio). The N₃-SAMs was immersed in an
277 ethanolic solution of 1.25 mM 4-(4-ethynylphenyl)-1-methylpyridin-1-ium iodide.
278 Additionally, solution of 0.4 mM CuSO₄·5H₂O and 0.8 mM ascorbic acid in deionized
279 water was added. Also, the samples were stored in a dark under a nitrogen atmosphere
280 for 2.5 days at 50 °C. After the completion of the reaction, we rinsed the samples with
281 ethanol and dichloromethane and the MPP+I-SAMs were obtained⁸.

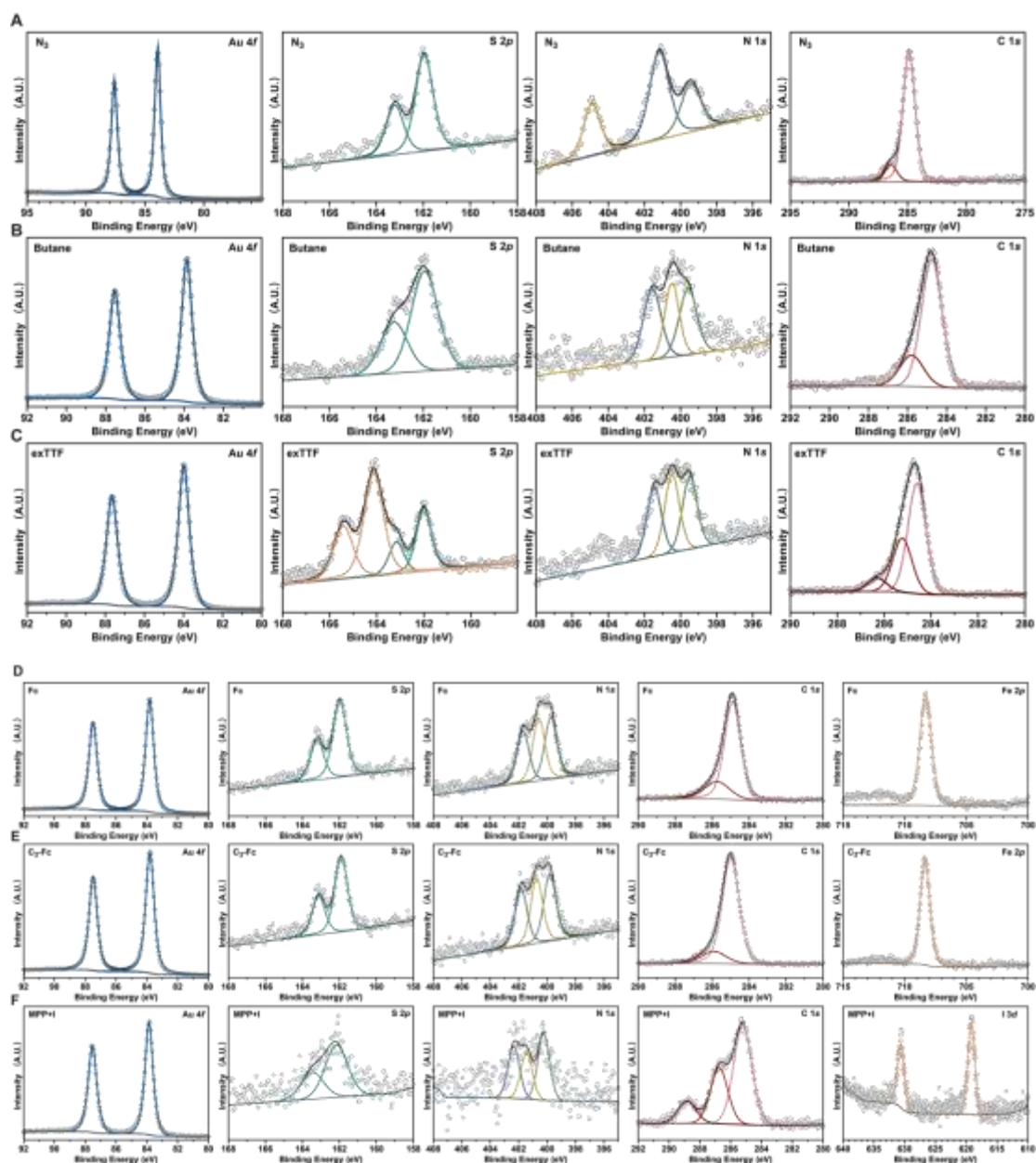
282

283 **3 X-Ray Photoelectron Spectroscopy & Ultraviolet photo-electron** 284 **spectroscopy**

285 X-ray photoelectron spectroscopy (XPS) was conducted with the NCESBJ
286 (National Centre of Electron Spectroscopy in Beijing). All measurements were
287 performed in an ultrahigh vacuum chamber with a base pressure of 1×10^{-8} Pa. The

288 energy of the incident X-ray beam (1486.6 eV) was used by the Thermo Scientific K-
 289 Alpha XPS system. To probe the valence band, the photon energy at 21.22 eV was used
 290 and -10 V bias was applied to the sample to overcome the work function of the analyzer.
 291 All UPS spectra were referenced to the Fermi edge of Au.

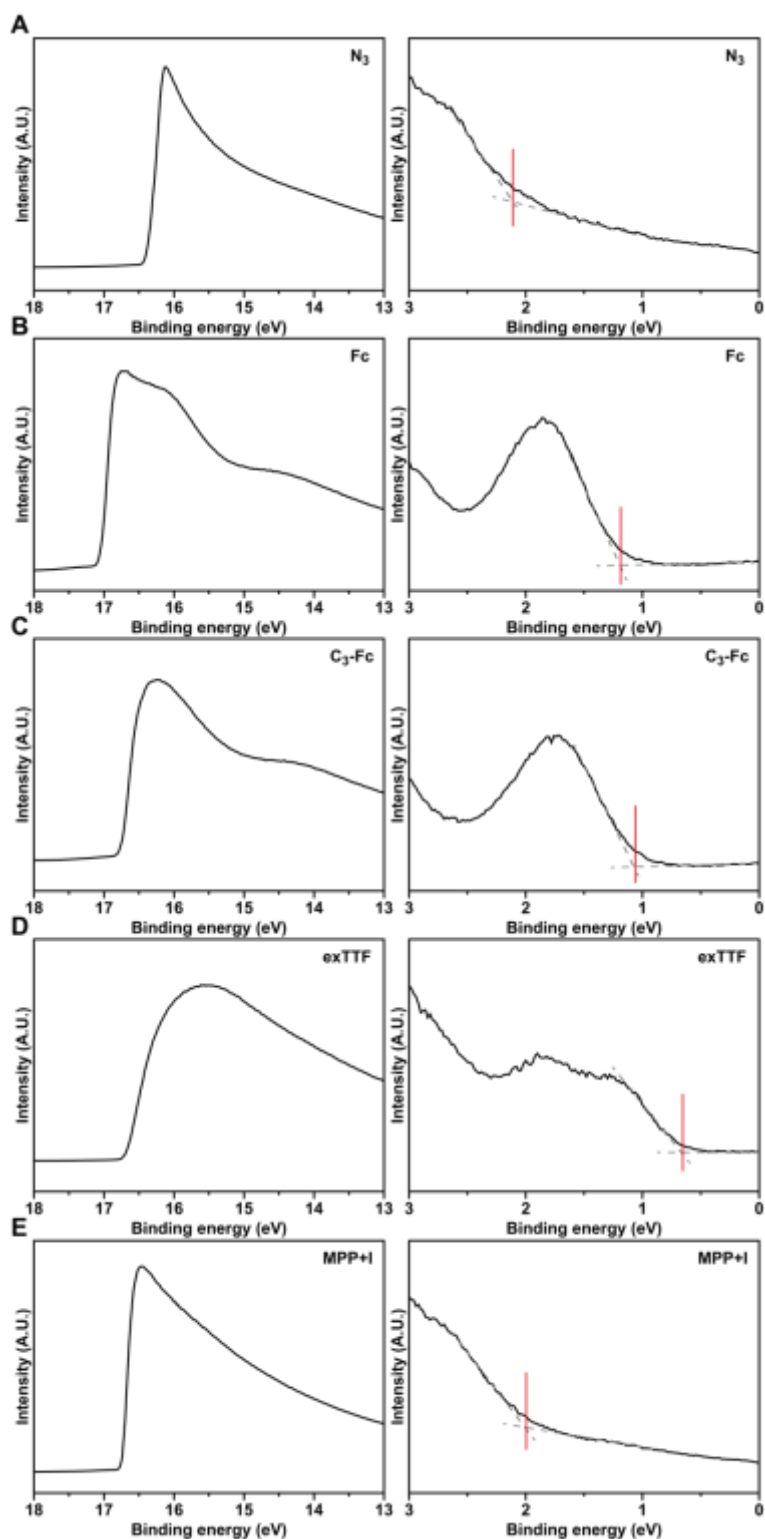
292



293

294

295 **Figure S32.** The XPS spectrum of all SAMs. (A) N₃; (B) Butane; (C) exTTF; (D) Fc;
 296 (E) C₃-Fc; (F) MPP-I



297

298 **Figure S33.** The UPS spectrum (Zoom-in to show work function and HOMO energy
 299 position) of all SAMs, referenced to the Fermi level of a clean polycrystalline Au
 300 surface. (A) N₃; (B) Fc; (C) C₃-Fc; (D) exTTF; (E) MPP-I

301

302

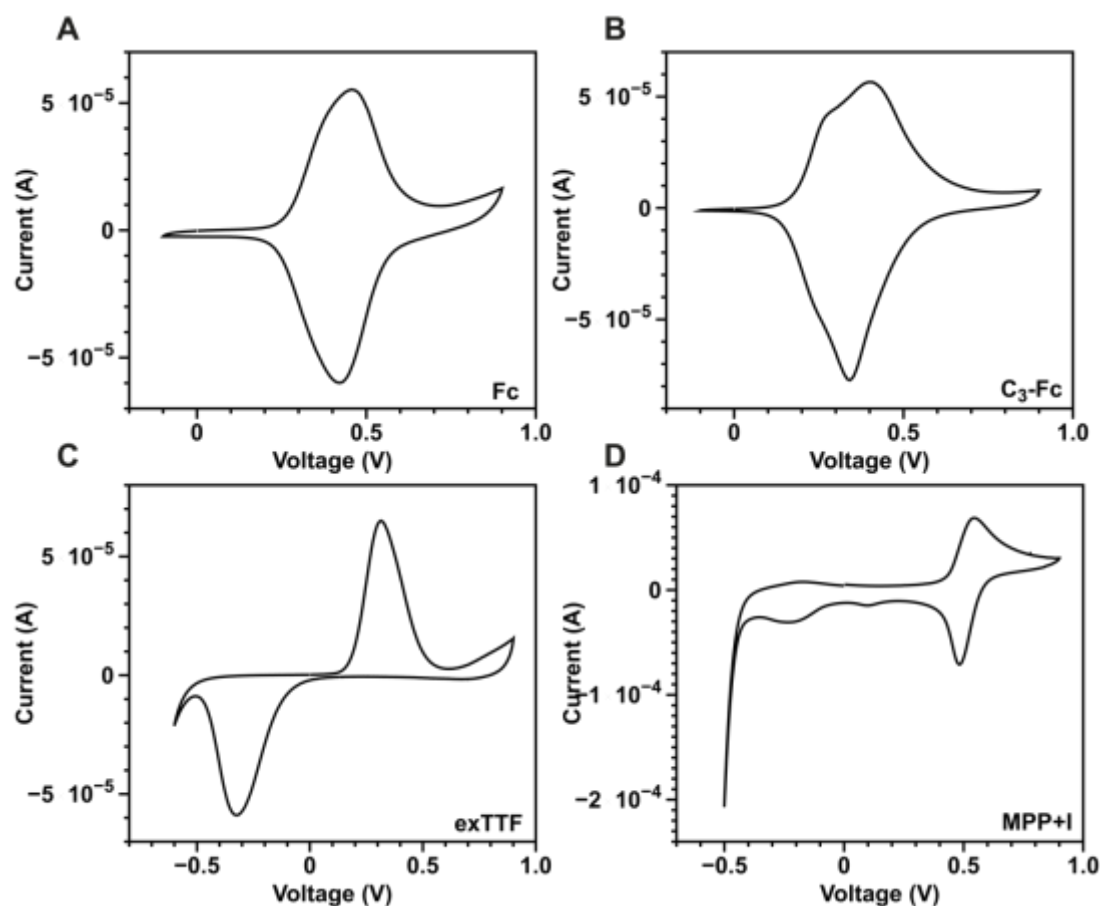
303 **4 Cyclic voltammetry**

304 The SAMs of all functional groups on Au^{TS} electrodes were electrochemically
305 characterized by cyclic voltammetry (CV)³. Electrochemical measurements were
306 performed with an AUTOLAB PGSTAT302N with NOVA 2.1 software. To perform
307 the CV measurements, we used a custom-built electrochemical cell equipped with a
308 platinum counter electrode, an Ag/AgCl reference electrode and the Au^{TS} film served
309 as a working electrode. Cyclic voltammograms were recorded in an aqueous solution
310 of 1.0 M HClO₄. The CVs were recorded in the range of −0.1 to +0.9 V for Fc and C3-
311 Fc; −0.4 to +0.9 V for exTTF and −0.5 to +0.9 V for MPP+I. We measured 3 substrates
312 for each SAMs.

313 We calculated the surface coverage (Γ , mol/cm²) with equation 1, where Q_{tot} is the
314 total charge obtained by integration of the CV, n is the number of electrons per mole of
315 reaction, F is the Faraday constant (96485 C/mol), and A is the surface area of the
316 electrode exposed to the electrolyte solution (0.65 cm²). The results are shown in Table
317 S1.

$$318 \quad \Gamma = Q_{\text{tot}}/nFA \quad (1)$$

319



320

321 **Figure S34.** The CV spectrum of all SAMs. (A) Fc; (B) C₃-Fc; (C) exTTF; (D)
 322 MPP+I

323 5 EGaIn measurement

324 We used cone-shaped tips of Ga₂O₃/EGaIn as the top electrodes following by a
 325 previously described home-built system³. This technique makes it possible to form
 326 junctions in which the electrical characteristics are dominated by the chemical and
 327 supramolecular structure of the SAMs inside the junctions and to record data with
 328 statistically large numbers. We have shown before that the device properties are not
 329 dominated by any of the other asymmetries, nor by the Ga₂O₃ layer, present in these
 330 junctions⁹.

331

332 6 Statistical analysis

333 For the freshly prepared SAMs, the junctions of each type of SAM were fabricated
 334 on three different Au samples using the ‘EGaIn-technique’. We formed seven junctions
 335 on each substrate. For each junction, we recorded 24 scans ($0\text{ V} \rightarrow +V_{\text{max}} \rightarrow 0\text{ V} \rightarrow -$
 336 $V_{\text{min}} \rightarrow 0\text{ V}$) with a step size of $V_{\text{max}}/20\text{ V}$ and a delay of 0.1 s. We collected large
 337 statistically large number of traces for each type of SAMs (see Table S2), and we
 338 calculated $\log|J|$ using previously reported methods³.

339

340 7 Molecular structure optimization

341 We optimized molecular geometry and molecular orbits (MOs) using the
 342 DFT/B3LYP function with basis set 6-31G (d) as implemented in Gaussian 09¹⁰.

343

344 **Table S1. Summary properties of the SAMs**

SAMs	UPS		CV			DFT	
	E_{HOMO} (eV)	WF (eV)	E_{pa} (mV)	E_{pc} (mV)	Γ ($\times 10^{-10}$ mol/cm ²)	HOMO (eV)	LUMO (eV)
Fc	-5.36	4.16	458	419	3.40	-5.08	-0.04
C3-Fc	-5.51	4.46	393	332	4.43	-5.07	0.16
TTF	-5.16	4.46	315	-320	1.93	-4.54	-1.22
MPP+I	-6.45	4.46	540	483	3.09	-7.08	-5.88
N ₃	-6.83	4.83	/	/	/	-6.35	-0.68

345

346 **Table S2. Yields of the click reaction**

SAMs	Γ ($\times 10^{-10}$ mol/cm ²)	Theoretical value ($\times 10^{-10}$ mol/cm ²)	Yields / %
Fc	3.40	4.50	75.5
C3-Fc	4.43	4.50	98.8
TTF	1.93	2.98	66.7
MPP+I	3.09	5.00	61.8

347 a

348

349

350

351

352

Table S3. Statistics for Au-SAMs//Ga₂O₃/EGaIn junctions.

	Number of Junctions	Number of shorts ^a	Number of traces ^b	Yields / (%) ^c
N ₃	21	0	504	100
Butane	21	0	504	100
Fc	21	0	504	100
C ₃ -Fc	21	0	504	100
exTTF	15	0	360	100
MPP+I	20	0	408	100

353 ^a A junction short was defined when the value of J exceeds 10^2 A/cm² (the upper limit of J
 354 measurable by our instrument) while recording 20 $J(V)$ scans.

355 ^b The number of $J(V)$ traces of the Au-SAMs/Ga₂O₃/EGaIn junctions.

356 ^c The yield is defined as the percentage number of non-shortening junctions divided by the
 357 total number of junctions.

358

359 8 References

- 360 1 L. Adamiak, J. Pendery, J. Sun, K. Iwabata, N. C. Gianneschi and N. L. Abbott,
 361 *Macromolecules*, 2018, **51**, 1978-1985.
- 362 2 Y. Y. Lin, S. C. Tsai and S. J. Yu, *J. Org. Chem.*, 2008, **73**, 4920-4928.
- 363 3 J. L. Lin, Z. Cao, X. Y. Bai, N. Y. Chen, C. T. Li, X. W. Xiao, L. J. Wang and Y.
 364 Li, *Adv. Mater. Interfaces*, 2022, **9**, 2201238.
- 365 4 R. Chen, Q. Weng, Z. An, S. Zhu, Q. Wang, X. Chen and P. Chen, *Dyes and*
 366 *Pigments*, 2018, **159**, 527-532.
- 367 5 L. Luo, J. Tang, R. Sun, W. Li, X. Zheng, M. Yuan, R. Li, H. Chen and H. Fu,
 368 *Org. Lett.*, 2022, **24**, 2821-2825.
- 369 6 W. Peng, Z. Cao, N. Chen, Y. Xie and Y. Li, *J. Mater. Chem. A*, 2022, **10**, 23304-
 370 23313.
- 371 7 S. Qiu, S. Gao, L. Xie, H. Chen, Q. Liu, Z. Lin, B. Qiu and G. Chen, *Analyst*,
 372 2011, **136**, 3962-3966.
- 373 8 E. Darlatt, C. H. H. Traulsen, J. Poppenberg, S. Richter, J. Kühn, C. A. Schalley
 374 and W. E. S. Unger, *J. Electron. Spectrosc. Relat. Phenom.*, 2012, **185**, 85-89.
- 375 9 C. A. Nijhuis, W. F. Reus and G. M. Whitesides, *J. Am. Chem. Soc.*, 2009, **131**,
 376 17814-17827.
- 377 10 M. J. Frisch, G. Trucks, H. B. Schlegel, G. E. Scuseria, Robb, J. R. Cheeseman, G.
 378 Scalmani, V. Barone, B. Mennucci and G. A. Petersson, 2009.
- 379